



## Review

# Road de-icing salt: Assessment of a potential new source and pathway of microplastics particles from roads



Elisabeth S. Rødland<sup>a,b,\*</sup>, Elvis D. Okoffo<sup>d</sup>, Cassandra Rauert<sup>d</sup>, Lene S. Heier<sup>c</sup>, Ole Christian Lind<sup>b</sup>, Malcolm Reid<sup>a</sup>, Kevin V. Thomas<sup>d</sup>, Sondre Meland<sup>a,b</sup>

<sup>a</sup> Norwegian Institute for Water Research, Gaustadalléen 21, N-0349 Oslo, Norway

<sup>b</sup> Norwegian University of Life Sciences, Center of Environmental Radioactivity (CERAD CoE), Faculty of Environmental Sciences and Natural Resource Management, P.O. Box 5003, 1433 Ås, Norway

<sup>c</sup> Norwegian Public Roads Administration, Construction, Postboks 1010, N-2605 Lillehammer, Norway

<sup>d</sup> Queensland Alliance for Environmental Health Sciences (QAEHS), The University of Queensland, 20 Cornwall Street, Woolloongabba, 4102, QLD, Australia

## HIGHLIGHTS

- Road de-icing salt is potentially a source of microplastic (MP) to the environment
- Rubber-like particles constituted 96% of the total concentration of MPs in road salt
- Eleven different polymers were confirmed present in road salt
- MP release was calculated based on road salt emissions in Norway, Sweden and Denmark
- Compared to other sources of MP from roads, contribution from road salt is negligible

## GRAPHICAL ABSTRACT

Illustration of road salt with microplastic particles released onto the roads. Illustrations created using Adobe Illustrator and free vectors from Freepik.



## ARTICLE INFO

## Article history:

Received 12 March 2020

Received in revised form 8 May 2020

Accepted 9 May 2020

Available online 2 June 2020

Editor: Damia Barcelo

## Keywords:

Plastic pollution

Salt

Road

FTIR

Pyrolysis-GC-MS

## ABSTRACT

Roads are estimated to be the largest source of microplastic particles in the environment, through release of particles from tires, road markings and polymer-modified bitumen. These are all released through the wear and tear of tires and the road surface. During the winter in cold climates, the road surface may freeze and cause icing on the roads. To improve traffic safety during winter, road salt is used for de-icing. Knowledge of microplastic (MP) contamination in road salt has, until now, been lacking. This is contrary to the increasing number of studies of microplastics in food-grade salt. The objective of this study was to investigate if road salt could be an additional source of microplastics to the environment. Fourier-Transform Infrared spectroscopy (FT-IR) and Pyrolysis gas chromatography mass spectrometry (GC-MS) were employed to identify and quantify the polymer content in four types of road salts, three sea salts and one rock salt. The particle number of MP in sea salts (range 4–240 MP/kg, mean  $\pm$  s.d. =  $35 \pm 60$  MP/kg) and rock salt (range 4–192 MP/kg,  $424 \pm 61$  MP/kg, respectively) were similar, whereas, MP mass concentrations were higher in sea salts (range 0.1–7650  $\mu\text{g}/\text{kg}$ ,  $442 \pm 1466$   $\mu\text{g}/\text{kg}$ ) than in rock salts (1–1100  $\mu\text{g}/\text{kg}$ ,  $322 \pm 481$   $\mu\text{g}/\text{kg}$ ). Black rubber-like particles constituted 96% of the total concentration of microplastics and 86% of all particles in terms of number of particles/kg. Black rubber-like particles appeared to be attributable to wear of conveyor belts used in the salt production. Road salt

\* Corresponding author at: Norwegian Institute for Water Research, Gaustadalléen 21, N-0349 Oslo, Norway.  
E-mail address: [elisabeth.rodland@niva.no](mailto:elisabeth.rodland@niva.no) (E.S. Rødland).

contribution to MP on state and county roads in Norway was estimated to 0.15 t/year (0.003% of total road MP release), 0.07 t/year in Sweden (0.008%) and 0.03 t/year in Denmark (0.0004–0.0008%) Thus, microplastics in road salt are a negligible source of microplastics from roads compared to other sources.

© 2020 The Authors. Published by Elsevier B.V. This is an open access article under the CC BY license (<http://creativecommons.org/licenses/by/4.0/>).

## Contents

1.	Introduction . . . . .	2
2.	Materials and method . . . . .	3
2.1.	Sample collection . . . . .	3
2.2.	Sample treatment . . . . .	3
2.3.	Visual analysis and FTIR . . . . .	3
2.4.	Pyrolysis GC–MS . . . . .	3
2.5.	Concentration calculations . . . . .	5
2.6.	Quality control and quality assurance . . . . .	5
2.7.	Emissions of MPs in road salt . . . . .	6
2.8.	Statistical analysis . . . . .	6
3.	Results . . . . .	6
3.1.	Quality control and quality assurance . . . . .	6
3.2.	Identification of MPs with FT-IR . . . . .	6
3.3.	Identification of MPs with Pyrolysis GC–MS . . . . .	7
3.4.	Particle measurements . . . . .	7
3.5.	Comparison of MPs between salt production sites . . . . .	9
3.6.	Comparison between salt types . . . . .	9
3.7.	Estimation of MP release from road salt . . . . .	9
4.	Discussion . . . . .	11
4.1.	Road de-icing salt compared to RAMP . . . . .	11
4.2.	Black rubbery particles . . . . .	11
4.3.	Comparison with other studies . . . . .	11
4.4.	Limitations of the methodology . . . . .	12
5.	Conclusions . . . . .	12
	Declaration of competing interest . . . . .	12
	Acknowledgements . . . . .	12
	Funding sources . . . . .	12
	Author contributions . . . . .	13
	Appendix A. Supplementary data . . . . .	13
	References . . . . .	13

## 1. Introduction

Microplastic pollution has gained a lot of attention the last few years, with an increasing number of studies detecting microplastic particles (MPs) in all types of environments (GESAMP, 2016). Although there has been a predominant focus on microplastics in marine environments, it has been suggested that the majority of the plastic contamination in the marine ecosystem comes from terrestrial sources (Andrady, 2011; Frias et al., 2016; Rochman, 2018). MPs are particles in the size range of 1 nm to <5 mm (GESAMP, 2016). In Norway, current estimates indicate a total annual emission of 8400 t of microplastic (Sundt et al., 2014), with an annual release of approximately 5500 t (Sundt et al., 2014; Sundt et al., 2016; Vogelsang et al., 2018) originating from the transport sector (Table S7). A significant proportion of this is expected to be able to reach the aquatic environment (Sundt et al., 2014). Car tire particles released from tire wear (TWP) have been proposed as the main source of MP particles generated on roads, with an annual emission of approximately 5000 t (Sundt et al., 2014; Sundt et al., 2016; Vogelsang et al., 2018). Similar assessments in Sweden and Denmark have also concluded that tires are the main source of microplastic particles from roads (Hann et al., 2018; Lassen et al., 2015; Magnusson et al., 2017; Sundt et al., 2014; Sundt et al., 2016). In addition to TWP, road wear particles from road markings (RWP<sub>RM</sub>) and polymer-modified bitumen (RWP<sub>PMB</sub>) have been identified as significant sources (Sundt et al., 2014; Sundt et al., 2016; Vogelsang et al., 2018). The yearly emission of RWP<sub>RM</sub> is estimated to be 100–300 t in

Norway, 500 t in Sweden and 700 t in Denmark. The annual emission of RWP<sub>PMB</sub> is estimated to be 30 t in Norway and 15 t Sweden (Sundt et al., 2014; Sundt et al., 2016; Vogelsang et al., 2018).

Until now, the application of road salt has not been addressed in terms of a source and pathway of microplastics to the environment. In cold climate regions, substantial amounts of road salt (sodium chloride, NaCl) is used for de-icing to maintain traffic safety during winter (Marsalek, 2003), and the amount of road salt used in several countries has increased dramatically since the 1950s (Schuler and Relyea, 2018). In the United States, approximately 1 million tonnes of road salt were applied in the 1950, and by 2017 this had increased with about 95%, to approximately 22 million tonnes of salt per year (Kelly et al., 2019; Schuler and Relyea, 2018, Table S1). Other countries with high road salt consumptions are Canada (7 million tonnes; Environment Canada, 2012) and China (600,000 t, Ke et al., 2013). The basis for this study is the emission of road salt in Norway, Sweden and Denmark, where 320,000 t, 210,000 t and 55,000 t of salt is used every year (Statens vegvesen, 2019a; Trafikverket, 2019; Vejdirektoratet, 2019a). Even though the total road salt consumption differs a lot between countries, so does the total length of their road network, from about 63,000 kilometer (km) in Norway (state and county roads) to 4.3 million km of paved roads in China (Table S1, CIA, 2017; Government of Canada, 2018; Statens vegvesen, 2019b; Trafikverket, 2017; US Department of Transportation, 2017; Vejdirektoratet, 2019b). Adjusting for the length of the road network, the salt consumption in both Norway and the United States is comparable and probably among the highest in the

world, with approximately 5 t of salt per km road (tonnes/km), with Canada on top with a consumption of over 6 t/km per year. In Sweden, the consumption is less than half of Norway and the United States, with about 2 t/km and in Denmark even lower, <1 t/km (Table S1, CIA, 2017; Government of Canada, 2018; Statens vegvesen, 2019b; Trafikverket, 2017; US Department of Transportation, 2017; Vejdirektoratet, 2019b).

Environmental concerns have arisen due to the amount of road salt applied in many countries, and it is now considered a major threat to freshwater systems in countries with temperate climates (Demers, 1992; Fay and Shi, 2012; Findlay and Kelly, 2011; Karraker et al., 2008; Tiwari and Rachlin, 2018). This is mainly due to the increasing salinity concentrations, which result in negative ecological effects on rivers, wetland and lakes, as well as threatening valuable drinking water. Recent studies have shown that food-grade salt can act as carrier for microplastic particles (MPs) (Gündoğdu, 2018; Iniguez et al., 2017; Karami et al., 2017; Kim et al., 2018; Lee et al., 2019; Seth and Shrivastav, 2018; Yang et al., 2015). Hence, the presence of MPs in salt used for de-icing purposes may also contribute to releases of MPs in the environment.

Several studies have identified MPs in both sea salt and rock salt used for food consumption (Gündoğdu, 2018; Iniguez et al., 2017; Karami et al., 2017; Kim et al., 2018; Lee et al., 2019; Seth and Shrivastav, 2018; Yang et al., 2015). The number of MPs found in food grade sea salt varies widely (n.d.–13,629 MP/kg), whereas the variation found for food grade rock salt is smaller (7–462 MP/kg). Sea salt originating from Asia, Oceania, Africa, South America, North America and Europe have been investigated, and in one of the studies (Kim et al., 2018) the number of MPs found in sea salt were significantly correlated to the number of MPs found in both rivers and seawater of areas where the sea salts are produced. The positive correlation between microplastics in sea salt and microplastics found in sea water has been discussed in several other studies (Gündoğdu, 2018; Lee et al., 2019; Seth and Shrivastav, 2018; Yang et al., 2015), as well as how urbanisation and human activities can potentially contaminate the sea salt at the production sites (Gündoğdu, 2018) in order to explain the variation found in the samples. The results of the food-grade studies indicate that sea salt is more contaminated with microplastics compared to rock salt, and that the sea water microplastic contamination can be transferred to sea salt. However, the presence of MPs in rock salts suggests contamination during production, transportation and packaging, indicating that salt also can act as a source of microplastics and not just a pathway of contaminated sea water.

The enormous quantity of road salt applied on roads during winter, together with recent understanding about MPs in food-grade salt therefore raised the question as to whether road salt could be a fourth significant source of MP in the environment from roads. The present study's main objective was to investigate if MP particles are present in road salt, and to estimate the potential emission of these MPs in Norway, Sweden and Denmark.

## 2. Materials and method

### 2.1. Sample collection

Salt used for de-icing purposes was provided by GC Rieber ([www.gcrieber-salt.no](http://www.gcrieber-salt.no)), which is the main salt distributor in Norway and Denmark. The sea salt originated from three different locations in the Mediterranean Sea: Torrevieja in Spain, and Zarziz and Ben Gardene in Tunisia (Fig. 1). One site of rock salt, originating from Bernburg, Germany, was also included in the study to be able to compare rock salt with the sea salt. The samples from Zarziz, Ben Gardene and Bernburg were between 2 and 5 kg, and were sampled directly from the salt piles at the GC Rieber storage unit at Sjørsøya in Oslo, Norway. The salt from Torrevieja was pre-packed as a food-grade salt for commercial sales in a 2-kg polyethylene (PE) bag, packed in Oslo (the

polymer type of the bag was tested in this study, see SI). The Torrevieja salt is the same salt used for road purposes. The salt from different locations was stored separately to avoid mixing.

### 2.2. Sample treatment

Sub-samples were taken from each of the salt sample bags, adding up to 250 g of salt. This was inserted in a 1000 mL bottle. Three technical replicates were taken from each salt sample. The subsampling took place in a sterile cabinet using a metal spoon to collect subsamples from different areas in the sample to total 250 g. To dissolve the salt, 1000 mL of filtered reverse osmosis (RO) water (0.22 µm membrane filters) was added to each bottle and the bottles were incubated at 60 °C and 100 rpm for 24 h. All bottles and equipment used in the laboratory analyses were rinsed with filtered RO water three times before use. To be able to identify any MPs present in the salt samples, the samples were filtered under vacuum onto glass fibre filters (Whatman GF/D, pore size 2.7 µm). For the sample prepared for Pyrolysis GC–MS, one technical replicate of 250 g of salt was taken from the sample and dissolved in 1000 mL filtered RO-water. Then a subsample of 500 mL of dissolved salt was filtered onto GF-filters (Whatman GF/A, 25 mm diameter, 1.6 µm pore size). All filters were placed in sealed petri dishes and dried at room temperature for at least one week.

### 2.3. Visual analysis and FTIR

The filters were examined using a stereomicroscope with Infinity 1-3C camera and INFINITY ANALYSE and CAPTURE software v6.5.6 to take pictures and to measure size (length, width and depth) of all particles found. For this study, the upper size limit is 5 mm (GESAMP, 2016) and lowest size limits are set by the pore size of the filters used for the Fourier-Transformed Infra-Red Spectrometry (FTIR)-analysis and the Pyrolysis gas chromatography mass spectrometry (GC–MS) (2.7 µm and 1.6 µm, respectively). Colour and morphology were also described for each particle. The categories for morphology were fibres, fibre bundles, fragments, spheres, pellets, foams, films and beads (Lusher et al., 2017; Rochman et al., 2019).

All particles considered by the visual inspection in stereomicroscope to be possible polymers were analysed using Fourier-Transformed Infra-Red Spectrometry (FTIR). The largest fragments (>200 µm) were analysed with single point measurement Attenuated Total Reflectance - Fourier Transformed Infra-Red Spectrometry (ATR-FT-IR) using a Cary 630 FT-IR Spectrometer from Agilent. Smaller particles (59–200 µm, longest axis) and all fibres were analysed with a FT-IR diamond compression cell in µ-transmission using a Spotlight 400 FT-IR Imaging system from Perkin Elmer. The particles were analysed with the full wavelength of the FT-IR (4000–600 cm<sup>-1</sup>) and resolution of 4 cm<sup>-1</sup>. The results were compared to the available libraries on each instrument. On the ATR-FT-IR, the results were compared to the Agilent Polymer Handheld ATR Library and the Elastomer O-ring and Seal Handheld ATR Library. On the FT-IR, the results were compared to the reference database from Primpke et al. (2018), the Perkin Elmer ATR Polymer Library and three inhouse reference libraries for rubbers, reference polymers and non-plastic particles. The spectra of all analysed particles were manually inspected. According to the methodology of Lusher et al. (2013) and recommended by the MSFD Technical Subgroup on Marine Litter (2013), only matches of 0.7 or above should be accepted. In this study we have included also matches between 0.7 and 0.6, as we have manually inspected all spectra.

### 2.4. Pyrolysis GC–MS

There were a large number of particles with rubber-like properties in the samples which could not be analysed using FTIR. Therefore, salt from the site where these particles were most abundant (Ben Gardene) were re-analysed using Pyrolysis GC–MS. The Pyrolysis GC–MS analysis was

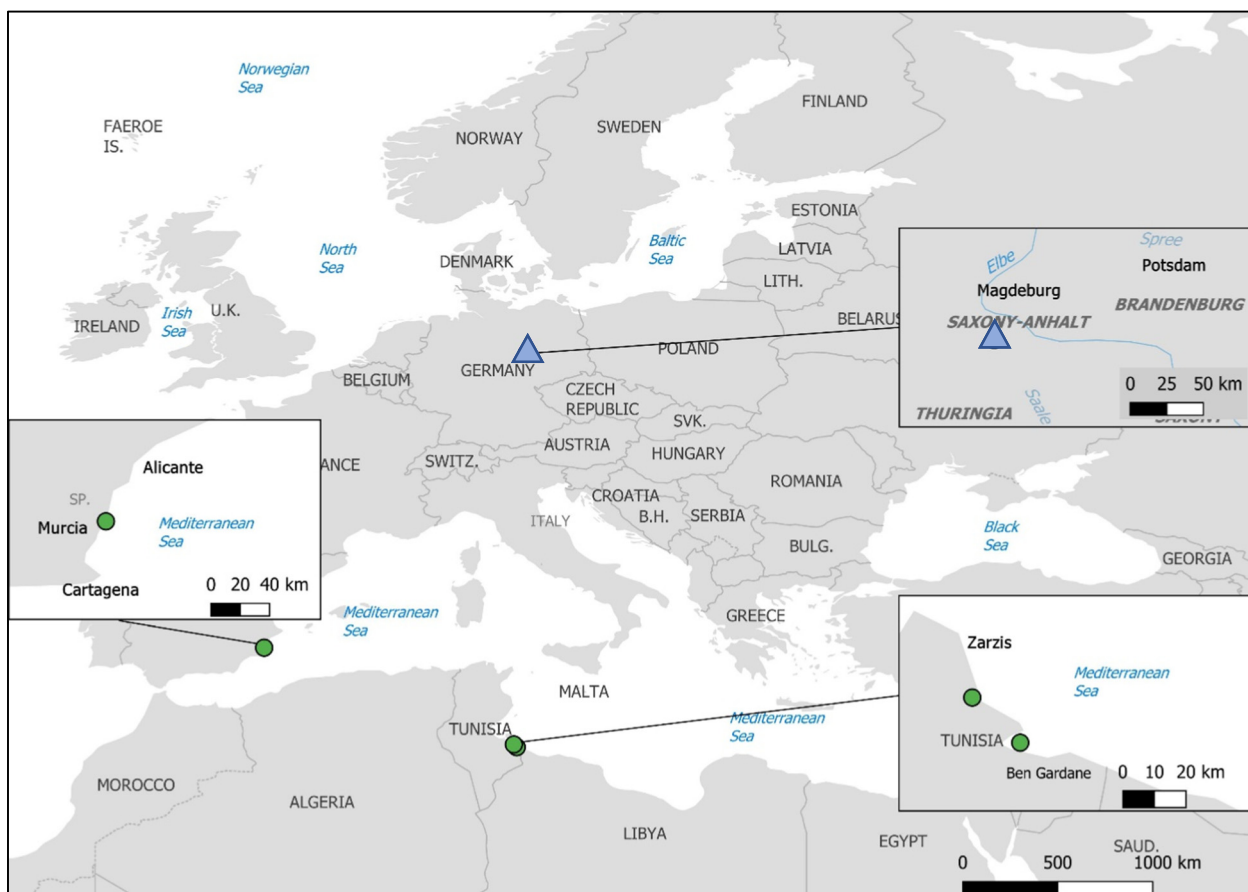


**Fig. 1.** Map over salt production sites Torrvieja (Spain), Zarzis and Ben Gardane (Tunisia) and Bernburg (Germany), created in QGIS (Natural Earth Package).

carried out using a multi-shot micro-furnace pyrolyzer (EGA/PY-3030D) with an auto-shot sampler (AS-1020E) (both Frontier Lab, Fukushima, Japan) attached to a Shimadzu Gas Chromatography–Mass Spectrometer (GC–MS) - QP2010-Plus (Shimadzu Corporation, Japan) equipped with an Ultra Alloy® 5 capillary column (Frontier Lab). Detailed Pyrolysis GC–MS conditions are summarized in Table 1.

**Table 1**  
Instrumental conditions for Pyrolysis–GC–MS measurements.

Apparatus	Parameters	Settings
Micro-furnace Pyrolyzer Frontier EGA/PY-3030D (Single-Shot analysis)	Pyrolyzer furnace/oven temperature	650 °C
	Pyrolyzer interface temperature	320 °C
Gas chromatogram (GC)	Pyrolysis time	0.20 min (12 s)
	Column	Ultra-Alloy® 5 capillary column (30 m, 0.25 mm I.D., 0.25 µm film thickness) (Frontier Lab)
	Injector port temperature	300 °C
	Column oven temperature program	40 °C (2 min) → (20 °C/min) → 320 °C (14 min)
	Injector mode	Split (split 50:1)
Mass spectrometer (MS)	Carrier gas	Helium, 1.0 mL/min, constant linear velocity
	Ion source temperature	250 °C
	Ionization energy	Electron ionization (EI); 70 eV
	Scan mode/range	Selected ion monitoring (SIM) mode, 40 to 600 m/z

To identify and quantify single polymers in samples, specific indicator ions were chosen by pyrolyzing polymer standards. The polymers analysed included PE (Sigma-Aldrich, St. Louis, MO, USA), Poly (methyl-methacrylate) (PMMA: Sigma-Aldrich, St. Louis, MO, USA), Polystyrene (PS: Sigma-Aldrich, St. Louis, MO, USA), Polyvinylchloride (PVC: Sigma-Aldrich, St. Louis, MO, USA), Polypropylene (PP: NIVA, Oslo, Norway), Polyethylene terephthalate (PET: Goodfellow, Cambridge, UK) and Polycarbonate (PC: NIVA, Oslo, Norway), as described and identified according to Okoffo et al. (2020), and also Styrene butadiene rubber (SBR) (SBR1500: Polymer Source, Quebec, Canada) (Table 2). For all polymers except for SBR, external calibration curves, ranging from 0.1 to 100 µg and having  $R^2 \geq 0.95$ , were obtained by extracting polymer standards with pressurized liquid extraction (PLE) (ASE 350, Dionex, Sunnyvale, CA) using dichloromethane (DCM) at 180 °C and 1500 psi, with a heat and static-time of 5 min using three extraction cycles. The final extract was analysed in an 80 µL pyrolysis cup (PY1-EC80F, Eco-Cup LF, Frontier Laboratories, Japan). For further PLE details and discussion including extraction parameters, recoveries and application, see Okoffo et al. (2020). For SBR, the external calibration curve ranging from 0.1 to 100 µg having  $R^2 = 0.99$ , was made in chloroform (Table 3), following the method described in the ISO method (ISO/TS 21396:2017, 2017).

To analyse for plastics, the 1.6 µm glass fibre filters used for the filtration of the samples were cut into three pieces with a pre-cleaned (with acetone and DCM) stainless steel scalpel, rolled and inserted into three pyrolysis cups for Pyrolysis–GC–MS analysis. Deuterated polystyrene (PS-d5; 216 µg/mL in DCM) and deuterated Poly(1,4-butadiene-d6) (7.6 mg/mL in chloroform) (both from Polymer Source, Inc., Quebec, Canada) were used as internal standards with 10 µL added directly to the calibration standards and samples in the cups, allowing the solvent to subsequently evaporate at room temperature.



**Table 2**  
Selected plastic indicator compounds. Italics and bold values used for calibration and quantification.

Plastic	Pyrolysis product	Indicator ions ( <i>m/z</i> )	Molecular ion ( <i>m/z</i> )	Retention time (min)	Calibration range ( $\mu\text{g}/\text{cup}$ )	LOD ( $\mu\text{g}/\text{kg}$ )	LOQ ( $\mu\text{g}/\text{kg}$ )	Linearity ( $R^2$ )
Polypropylene (PP)	2,4-Dimethyl-1-heptene	70, 83, <b>126</b>	126	4.53	0.2–100	0.90	2.72	0.98
Polystyrene (PS)	5-Hexene-1,3,5-triyltribenzene (styrene trimer)	<b>91</b> , 117, 194, 312	312	15.80	0.1–100	0.61	1.84	0.97
Poly-(methyl methacrylate) (PMMA)	Methyl methacrylate	69, <b>100</b> , 89	100	2.95	0.4–100	1.58	4.80	0.99
Polyethylene terephthalate (PET)	Vinyl benzoate	<b>105</b> , 77, 148, 51	148	7.61	0.3–100	1.42	4.31	0.99
Polycarbonate (PC)	Bisphenol A (BA)	<b>213</b> , 119, 91, 165, 228	228	14.52	0.5–100	1.90	5.74	0.95
Polyethylene (PE)	1-Decene (C10)	<b>83</b> , 97, 111, 140	140	6.22	0.2–100	0.93	2.83	0.97
Polyvinyl chloride (PVC)	Benzene	<b>78</b> , 74, 52	78	2.44	0.4–100	1.98	6.00	0.96
Styrene butadiene rubber (SBR)	4-Vinylcyclohexene	39, <b>54</b> , 79, 108	108	4.36	0.1–100	1.71	5.18	0.99
Internal standard								
Polystyrene-d5	Styrene-d5	<b>109</b> , 82, 54, 107		5.10				
Poly(1,4-butadiene-d6)		<b>60</b> , 120, 42, 86		4.28				

## 2.5. Concentration calculations

Length, width and depth of each particle were used to calculate the volume of the particle. This has been done in a few studies before, in order to obtain the concentrations of particles (Hermabessiere et al., 2018; Kim et al., 2018; Simon et al., 2018). For some particles, the depth was difficult to measure in the microscope due to the small size and irregular shape of the particle (fragments). For these particles, the depth was determined by width/2. Previous studies have assumed that the ratio between the depth and the width is the same as the ratio between the width and the length of a particle (Simon et al., 2018). Using the same approach, we determined the mean ratio of width and length for all MP fragments found in the salt sample to be  $0.4 \pm 0.4$ . For simplification purposes, we have assumed that all fragments have a depth which corresponds to 50% of the width of the particle. For the particles with confirmed polymer matches, the volume of the particle and the density of the polymer type was used to calculate mass of each particle.

## 2.6. Quality control and quality assurance

To avoid contamination in the process of sample treatment to analysis, a clean, enclosed lab designed for microplastic analysis was used throughout the study. Lint removal were used on the cotton laboratory coats before working in the lab, and all glassware and equipment were washed and rinsed with filtered RO-water. For each day of sample filtration (2.5 days), control samples (1000 mL filtered RO water in 1000 mL bottles) were filtered ( $n = 3$  for days 1 and 2,  $n = 2$  for third day).

As we have chosen to only focus on polymer particles found in road salt, i.e. excluding the natural and semisynthetic particles, only the

confirmed polymers (match >0.6) is used to calculate the Limit of Detection (LOD) and the Limit of Quantification (LOQ). LOD and LOQ are indicators used to explain the detectable limits of the method (i.e. the lowest concentration that is detectable) and the concentrations that can be quantified in samples, respectively. These two indicators are used in instrumental analysis of organic compounds, especially when using GCMS to report the detectable and quantifiable limits. For the samples analysed with visual inspection and FT-IR, we calculated the LOD and LOQ using the mean number of particles ( $\mu x$ ) and the standard deviation ( $\sigma x$ ) in the following equations:

$$LOD = \mu x + (\sigma x * 3) \quad (1)$$

$$LOQ = \mu x + (\sigma x * 10) \quad (2)$$

For the samples analysed with Pyrolysis GC-MS, the LOD and LOQ for each polymer was calculated by multiplying the standard deviation ( $\sigma x$ ) of 7 replicate injections of the lowest calibration standard spiked on a 1.6  $\mu\text{m}$  glass fibre filter with 3.3 and 10 respectively. LOD and LOQ values were then divided by the weight (kg) of sample (Table 3).

$$LOD = \sigma x * 3.3 \quad (3)$$

$$LOQ = \sigma x * 10 \quad (4)$$

Each Pyrolysis GC-MS run featured a calibration standard check and a blank (clean pyrolysis cup) every ten sample injections. Instrument blanks (no pyrolysis cup) were run between each batch of samples to avoid cross contamination, and a quality control and quality assurance sample (QAQC) sample was injected at the beginning and end of each run.

**Table 3**  
Comparison between polymer concentrations found in the sample from Ben Gardene using calculated mass of each particle and using Pyrolysis GC-MS for bulk concentration, MP per kilo ( $\mu\text{g}/\text{kg}$ ). Polymer types: polyethylene terephthalate (PET), polyethylene (PE), polyvinyl chloride (PVC), polypropylene (PP), Poly(methyl methacrylate) (PMMA), Polycarbonate (PC) and Styrene Butadiene Rubber (SBR).

Site	Polymer	Estimated (visual + FT-IR) $\mu\text{g}/\text{kg} \pm \text{s.d.}$	Measured (Pyrolysis GC-MS) $\mu\text{g}/\text{kg}$
Ben Gardene	PS	Not detected	6.0
Ben Gardene	PP	Not detected	13.8
Ben Gardene	PET	126.4 $\pm$ 173.3	105.5
Ben Gardene	BRP (PVC/SBR)	4463.6 $\pm$ 2759.7	-
Ben Gardene	PVC	-	1754.3
Ben Gardene	SBR	-	87.3
Ben Gardene	PE	116.8	302.3
Ben Gardene	PMMA	Not detected	Not detected
Ben Gardene	PC	Not detected	Not detected

## 2.7. Emissions of MPs in road salt

To compare the emission of MPs from road salt to the emissions of RAMP in Norway, Sweden and Denmark, the mean calculated concentrations of microplastics for each salt type (sea salt or rock salt) was multiplied with the amount of road salt released in each country. The amount and type of road salt used in Norway, Sweden and Denmark differs greatly. The amount of salt used is mainly dependent on the weather conditions of each winter season and might therefore fluctuate between years. However, the trend for the past 15 years shows an increase in the salt consumption on state and county roads in Norway (Fig. 2). According to the Norwegian Public Roads Administration (Statens vegvesen, 2019a), both the change in weather conditions (increased number of days with temperatures fluctuating around 0 °C), and the expansion of road networks is responsible for this increase. In Sweden, the salt consumption has followed a negative trend since 2007 compared to the amount used in 2003–2006, and for the last 4 years Sweden has used close to half the amount of road salt that was used on state and county roads in Norway. In Denmark, only data from 2011 to 2018 was available. Compared to Norway and Sweden, the salt consumption in Denmark is considerably lower.

## 2.8. Statistical analysis

The descriptive statistical analysis of the data was conducted in RStudio 1.2.5001 (RStudio, 2019), using the ggplot-package (Wickham, 2009) for graphic display of the dataset. The multivariate statistical analysis of this study includes a constrained redundancy analysis (RDA) and was conducted in Canoco 5.12 (Braak and Šmilauer, 2018). RDA was used to assess any differences in amount and composition of MPs between sites and salt type. The data used for these tests were number of particles for each polymer type found in the samples, and percentage of concentration of each polymer found in the samples.

The explanatory variables (categorical variables) were sample sites and the two salt types: sea salt and rock salt. All data was log transformed prior to the RDA and Monte Carlo permutation test (4999 permutations) were used for all tests. A probability (p) value of 0.05 was applied to all statistical tests.

## 3. Results

### 3.1. Quality control and quality assurance

In total, 8 fibres were found in the blank control samples and no fragments. All fibres were checked with the FT-IR and 5 fibres had a confirmed match with the database: two cellulose, two viscose wool and one polyethylene terephthalate (PET). Only the confirmed PET fibre is used to calculate LOD and LOQ: the mean number of fibres ( $\mu x$ ) was 0.1 with 0.4 as the standard deviation ( $\sigma x$ ), which gives a LOD of 1.3 and LOQ = 4.1. The calculated mean concentration of microplastic particles in the blank control samples were 0.07  $\mu g$  (with 0.2 as the standard deviation) which gives LOD = 0.7  $\mu g$  and LOQ = 2.1  $\mu g$ . All samples were filtered on the same day as the control sample with the PET fibre is corrected for the mean PET value, which included all the samples from Torrevieja.

The LOD for the pyrolysis method was between 0.61 and 1.98  $\mu g/kg$ , and the LOQ was between 1.84 and 6  $\mu g/kg$ . The value for each polymer is listed in Table 2.

### 3.2. Identification of MPs with FT-IR

In total, 608 particles were identified as potential microplastics following visual identification. Of these, 374 were classified as fragments, 230 as fibres, and 2 as spheres. For the fragments, particles  $\geq 59 \mu m$  were analysed with FT-IR. All non-black fragments ( $n = 51$ ) were analysed, and 27 of these were confirmed to be microplastics and 3

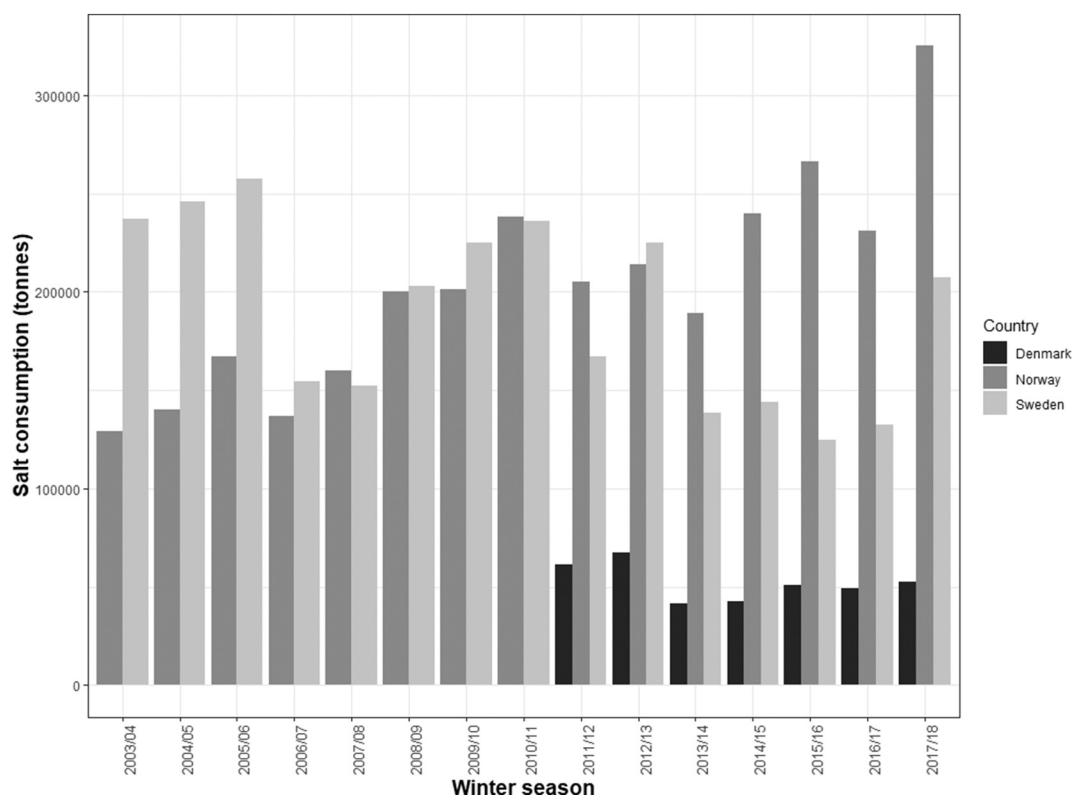


Fig. 2. The amount of road salt (tonnes) used on state and county roads in Norway (Statens vegvesen, 2019a, 2019b), Sweden (Trafikverket, 2019) and Denmark (Vejdirektoratet, 2019a, 2019b) from the winter season of 2003/04 to 2017/2018.

confirmed to be from natural sources (linen and viscose). Nitrile butadiene (NR, 22%) and PET (18%) were the most abundant non-black fragments. A total of 21 non-black fragments were unidentified or had a low match score ( $<0.6$  match) with the database.

The most abundant particle group in the samples were black fragments, collectively named “black rubbery particles” (BRP,  $n = 319$ ). They could all be placed in two morphology-groups, square-like or elongated (Fig. 3) and there was no visible difference between BRP from different salt sites. All had a “rubbery” response to pressure with the forceps and did not crumble or disintegrate, and therefore suspected to be made of polymeric material. Of the 319 B.P. found in the samples combined, 57 B.P. were subjected to FT-IR analysis. Out of these 57, only 20 particles had a match to the database ( $>0.6$ ); the spectra obtained matched that of reference tire samples - spectra showing the full absorbance of the Germanium crystal due to high carbon black content in tires. However, this result only shows us that the particle has a high carbon black content and does not confirm that they are all tire particles. The remaining 37 B.P. that were tested, could not be identified with respect to polymer type. Tires can contain different polymers, such as Styrene Butadiene Rubber (SBR), Butadiene Rubber (BR) and natural rubber, and tire particles are therefore included in the term microplastic. However, most of the particles found in this study did not seem to match the shape of tire particles reported from other studies (Kreider et al., 2010). Another source of black material with high content of carbon black was suggested, namely conveyer belts. Conveyer belts used in mining, for transporting material on site, are made of Polyvinyl chloride (PVC) (Van and Ter, 1990). To confirm that these numerous black particles could originate from conveyer belts, a new sub-sample of salt from Ben Gardene was analysed using Pyrolysis GC-MS.

Of the fibres detected, 194 were analysed by FT-IR. Unfortunately, 34 fibres were either lost during the transfer from filter paper to diamond compression cell or too small to be transferred. A total of 87 fibres had a

confirmed database match (match  $> 0.6$ ). Of these, 11 were confirmed to be microplastics, and 74 fibres were confirmed to be of natural material (cellulose = 68, wool = 5, cotton = 1) and 9 of semisynthetic material (viscose). 98 fibres were either unidentifiable or had a low match score with the database (match  $< 0.6$ ). The two spheres were also analysed using FT-IR and had no confirmed match with the database for any material.

### 3.3. Identification of MPs with Pyrolysis GC-MS

The presence of PVC in the samples from Ben Gardene was confirmed using Pyrolysis GC-MS. While PMMA and PC was not detected in the sample, the other 6 polymers were all above the detection limit and confirmed to be present in the road salt from Ben Gardene. Polyvinyl chloride accounted for 77% of the total polymer content found in the sample, followed by PE (13%), PET (5%), SBR (4%), PP (0.6%) and PS (0.3%). The presence of 4% SBR indicates that some of the BRP found in the salt samples were likely tire particles, at least in the samples from Ben Gardene. However, since we did not manage to distinguish between them in the visual analysis, we will for this study keep the term BRP as a combined group of PVC and SBR.

### 3.4. Particle measurements

The length of fragments, measured at the longest axis, ranged from 21  $\mu\text{m}$  to 2849  $\mu\text{m}$  ( $215 \pm 229 \mu\text{m}$ ) for all samples, and most of the fragments were smaller than 200  $\mu\text{m}$  (62%) and only 1% were larger than 1000  $\mu\text{m}$ . The length of fibres ranged from 126  $\mu\text{m}$  to 4800  $\mu\text{m}$  (mean  $\pm$  s.d. =  $1266 \mu\text{m} \pm 1197 \mu\text{m}$ ) in all salt samples (4). A large proportion of the fibres (45%) were longer than 1000  $\mu\text{m}$  and in total only 14% were smaller than 200  $\mu\text{m}$ .

The mass of both fragments and fibres was calculated from the volume of each particle and density of the polymer type that was

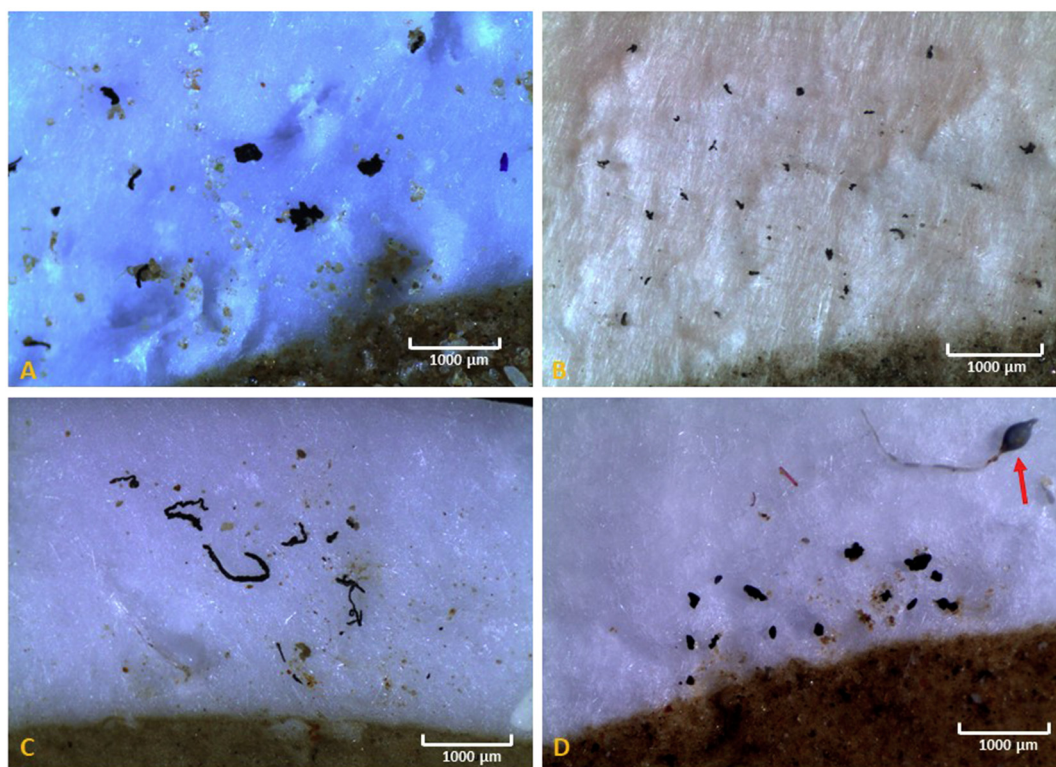


**Fig. 3.** Examples of black rubber-like particles (BRP) from samples A) Ben Gardene, B) Torrvieja, C) Zarziz and D) Rock salt from Bernburg, Germany. Image D also displays one of the two spheres found in the samples (highlighted with a red arrow). Images are taken with Infinity 1-3C camera and processed with INFINITY ANALYSE and CAPTURE software (v6.5.6).

confirmed for each, following the description of Subsection 2.5. The mass of fragments ranged from 0.03  $\mu\text{g}$  to 550  $\mu\text{g}$  ( $11 \pm 38 \mu\text{g}$ ), with as much as 78% of all fragments being  $<10 \mu\text{g}$ . Comparing the average values of both length and mass for all particles to the median values, it is quite clear that the sizes of MPs found in this study is skewed (Fig. 4), with a few large particles and most of them smaller than 200  $\mu\text{m}$  and with mass lower than 50  $\mu\text{g}$ . The concentrations of fibres ranged from 0.03  $\mu\text{g}$  to 80  $\mu\text{g}$  ( $5 \pm 15 \mu\text{g}$ ) in all samples. More than half of the fibres (52%) were  $<1 \mu\text{g}$  and 45% were between 1 and 10  $\mu\text{g}$ .

The calculation of the masses was controlled by comparing the results with the measured concentration using the Pyrolysis GC-MS from the Ben Gardene site (Table 3). At Ben Gardene, only PET and PEE particles were confirmed using FT-IR and the estimated concentration based on the particles detected was  $126 \pm 173 \mu\text{g}/\text{kg}$  and  $117 \mu\text{g}/\text{kg}$ , respectively. The largest group detected in the Ben Gardene sample was the BRP. If we assume that the BRP are PVC-particles from conveyer belts, as suggested in Subsection 3.2, the estimated concentration of BRPs is  $4464 \pm 2760 \mu\text{g}/\text{kg}$ . Using Pyrolysis GC-MS, the concentration

of PET, PVC, PE and SBR was measured to be 106  $\mu\text{g}/\text{kg}$ , 1754  $\mu\text{g}/\text{kg}$ , 302  $\mu\text{g}/\text{kg}$  and 87  $\mu\text{g}/\text{kg}$ , respectively. The presence of SBR in the samples suggests that some of the particles in the BRP group are tire particles and not PVC-particles. According to previous studies, the polymer content (both synthetic and natural) in tires is between 40 and 60% (Wik and Dave, 2009) and includes SBR, Polybutadiene, Polyisoprene, Chloroprene, natural rubber and other rubbers (Grigoratos and Martini, 2014; Wagner et al., 2018). The average SBR content of tires, combining car and truck tires, is 11.3% (Eisentraut et al., 2018). Assuming a 11.3% SBR content in tires, the total tire particle concentration in the sample is 773  $\mu\text{g}/\text{kg}$ . The visual analysis cannot differentiate between the possible conveyer belt particles and the tire particles, so using only visual techniques both particle types would be mixed. If we also combine the concentration for PVC and the calculated tire concentration based on the measured SBR concentration (using 11.3% SBR/tire) from the pyrolysis, the concentration of these two would add up to 2527  $\mu\text{g}/\text{kg}$  salt, which is within the range of concentration found for BRP using the visual analysis and concentration calculations.

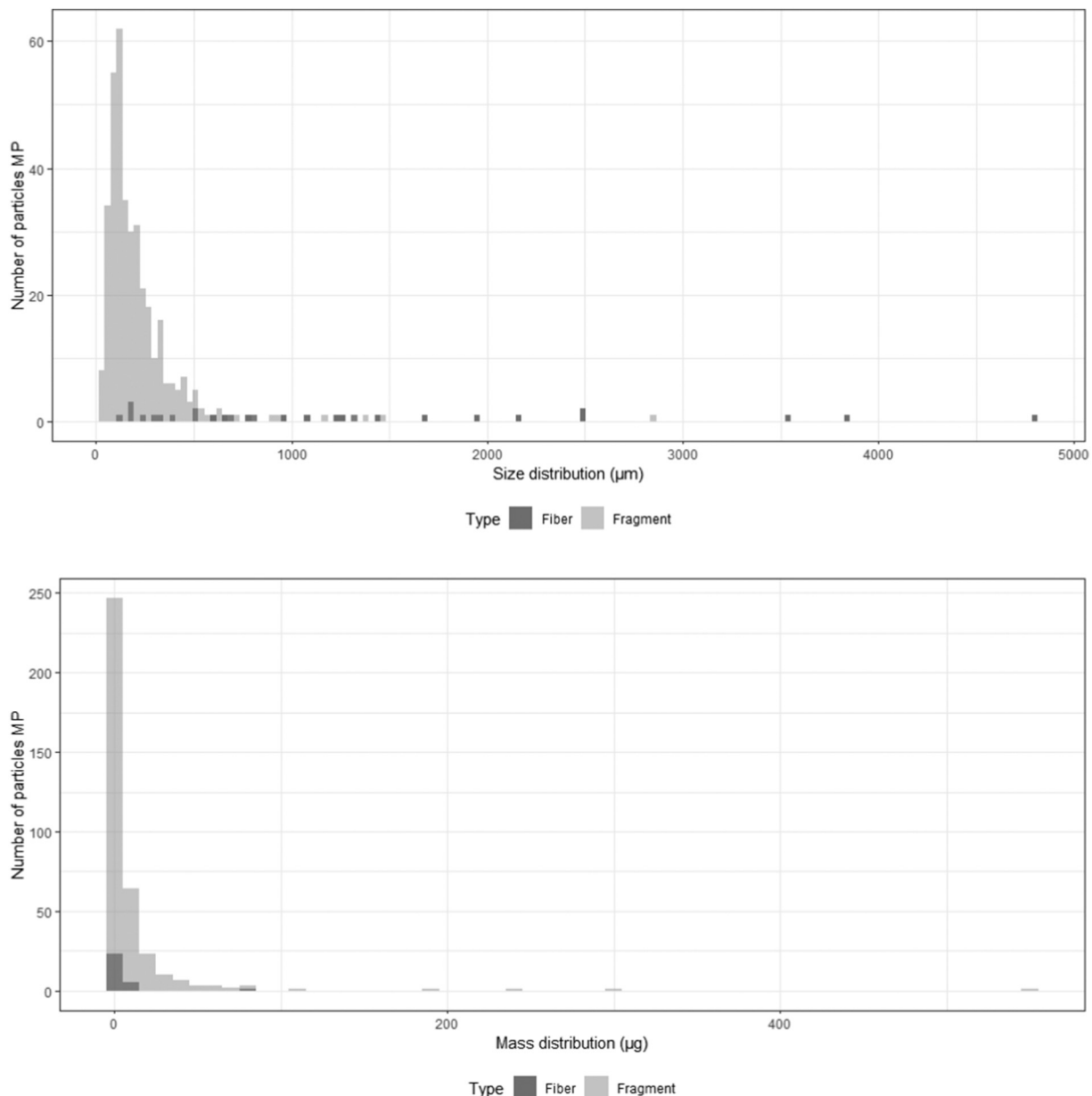


Fig. 4. Bar plot showing size (above) and the mass (below) distribution of all MPs found in the salt samples combined. Fibres and fragments are separated.



### 3.5. Comparison of MPs between salt production sites

The number of MPs found varied between samples, from 32 to 252 MP/kg (mean  $\pm$  s.d. =  $132 \pm 63$  MP/kg;  $n = 12$ , Table S2). The concentration of microplastic particles varied between samples from 1.5 to 3987  $\mu\text{g}/\text{kg}$  (mean  $\pm$  s.d. =  $595 \pm 1129$ ;  $n = 12$ , Table S3). Fragments were the most abundant type of particles in the samples, with 24–240 fragments per sample (mean  $\pm$  s.d. =  $122 \pm 64$  MP/kg;  $n = 12$ ) compared to 4–16 fibres per sample (mean  $\pm$  s.d. =  $10 \pm 3$  MP/kg). Comparing the concentrations per sample, the highest concentrations were also identified from the fragments, with an average of 1359  $\mu\text{g}/\text{kg}$  (s.d.  $\pm$  2251  $\mu\text{g}/\text{kg}$ ) compared to 49  $\mu\text{g}/\text{kg}$  (s.d.  $\pm$  93  $\mu\text{g}/\text{kg}$ ) for the fibres.

The samples from Ben Gardene contained a relatively high amount of fragments (mean  $\pm$  s.d. =  $4503 \pm 2725$   $\mu\text{g}/\text{kg}$ ; 195 MP/kg  $\pm$  41) compared to all the other sites: Torrevieja (mean  $\pm$  s.d. =  $173 \pm 103$   $\mu\text{g}/\text{kg}$ ; 107 MP/kg  $\pm$  20), Zarziz (mean  $\pm$  s.d. =  $24 \pm 31$   $\mu\text{g}/\text{kg}$ ; 52 n/kg  $\pm$  33) and Bernburg (mean  $\pm$  s.d. =  $735 \pm 503$   $\mu\text{g}/\text{kg}$ ; 136 MP/kg  $\pm$  60) (Fig. 5, Tables S4 & S5). For all sites, the number of fibres found per sample was considerably lower than the number of fragments. Torrevieja had the highest number of fibres (mean  $\pm$  s.d. =  $13 \pm 3$  MP/kg,  $n = 3$ ) compared to Zarziz (mean  $\pm$  s.d. =  $11 \pm 2$  MP/kg), Ben Gardene (mean  $\pm$  s.d. =  $9 \pm 2$  MP/kg), and Bernburg (mean  $\pm$  s.d. =  $8 \pm 5$  MP/kg), although all sites were quite similar in number of fibres found. However, when we use the concentration data, the concentration of fibres from the Ben Gardene site (mean  $\pm$  s.d. =  $128 \pm 172$   $\mu\text{g}/\text{kg}$ ,  $n = 3$ ) had four times higher concentration than Torrevieja (mean  $\pm$  s.d. =  $32 \pm 6$   $\mu\text{g}/\text{kg}$ ), five times higher than the Bernburg (mean  $\pm$  s.d. =  $24 \pm 6$   $\mu\text{g}/\text{kg}$ ) and 64 times higher concentration than Zarziz (mean  $\pm$  s.d. =  $2 \pm 1$   $\mu\text{g}/\text{kg}$ ).

### 3.6. Comparison between salt types

When comparing the types of road salt, the results indicate that sea salts have a higher concentration of MPs ( $442 \pm 1466$   $\mu\text{g}/\text{kg}$ ), and a larger variation in the samples compared to the rock salt ( $322 \pm 481$   $\mu\text{g}/\text{kg}$ ). However, the rock salts have the highest number of particles ( $61 \pm 76$  MP/kg) compared to the sea salts ( $35 \pm 60$  MP/kg). All data are summarized in Tables S1–S2.

The polymers identified differed between the samples. However, the most abundant particle-type found in all four sites were the BRP, which we have confirmed to consist of PVC and SBR (Fig. S4, Tables S4 & S5).

These were both the most numerous particles, as well as highest in concentration, and in fact accounted for 96% of the total MP (MP/kg) found in the samples combined, with confirmed PET at a second place (3%) and the rest accounts for 1% combined (Acryl A, Epoxy Resin ER, Ethylene Propylene EP, PEE, PVC (non-black), High-density Polyethylene (HDPE), Nitrile butadiene (NR), Polyurethane (PUR) acrylic resin, Polypropylene (PP)). Even though the BRP were the most abundant group at all sites, they were clearly found in the highest concentration at Ben Gardene (13,391  $\mu\text{g}/\text{kg}$ ; 580 MP/kg) and at Bernburg (2196  $\mu\text{g}/\text{kg}$ ; 400 MP/kg) (Fig. 6). The only other polymer found at all sites were PET fibres. Other detected polymers had greater variation between sites. One of the sites, Zarziz, had considerably more diverse particles than the others, with three different fibre polymers (A, PEE, PET) and six different fragment polymers (EP, NR, PET, PP, PVC and BRP) found.

The polymer type composition in the various salts appeared slightly different. However, using sampling sites as categorical variables in an RDA on both number of particles (pseudo-F = 2.0,  $p > 0.05$ ) and % concentration data (pseudo-F = 2.1,  $p > 0.05$ ) revealed no statistically significant difference in composition between sites (Fig. 7, Figs. S5 & S6). For the number of particles and concentration data, the sites explained 33% and 23.3% of the observed variation, respectively. The distance in the RDA between the two sites Ben Gardene and Bernburg is considerably lower when using concentration data compared to number of particles in 3a. There was, however, no significant difference found between the two salt types; sea salt and rock salt (MP/kg, pseudo-F = 0.9,  $p > 0.05$ ; MP g/kg, pseudo-F = 0.7,  $p > 0.05$ , see Figs. S5 & S6).

### 3.7. Estimation of MP release from road salt

For the calculations of MP release from road salt, the latest dataset from 2017/2018 is used. In this period, Norway used 320,000 t (Fig. 2) (Statens vegvesen, 2019a), distributed on about 50% sea salt produced in the Mediterranean and 50% rock salt produced in salt mines in Germany. Sweden only used rock salt on their state and county roads, and for the season 2017/2018, close to 210,000 t of salt was used (Trafikverket, 2019). In Denmark, 55,000 t of salt were used in the whole of 2018, and only sea salt from the Mediterranean was used (Vejdirektoratet, 2019a). The average concentration of MPs in the sea salt was 442.1  $\mu\text{g}/\text{kg}$  salt and the average number of particles was 35.1 MP/kg. The average concentration of MPs in the rock salt was 321.8  $\mu\text{g}/\text{kg}$  and the average number of particles was 60.5 MP/kg. Even though

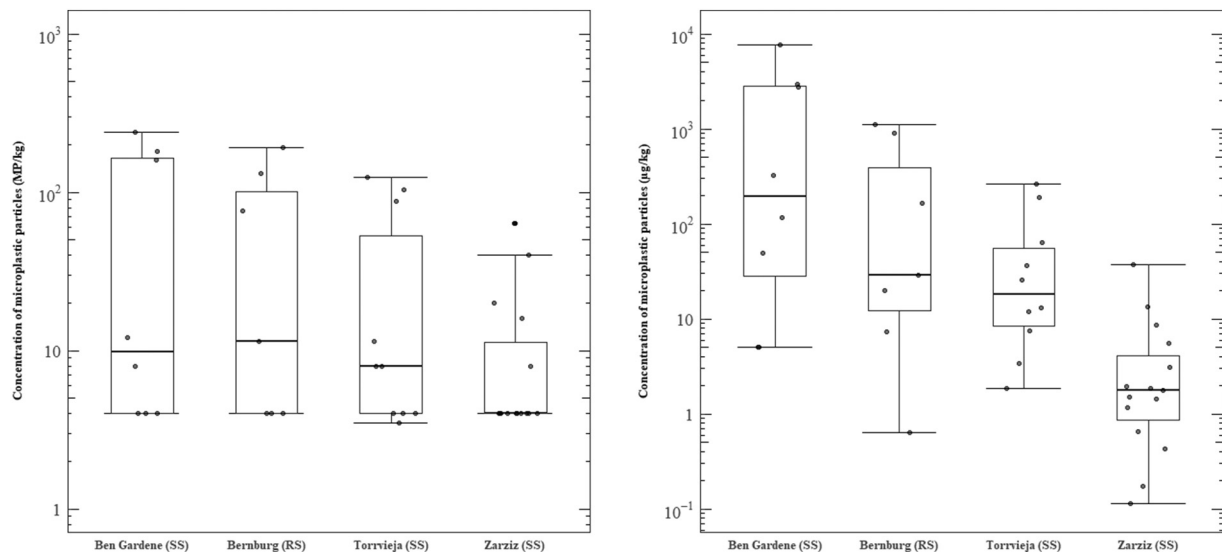


**Fig. 5.** Box plot showing the spread of microplastic particles found throughout the samples analysed, depicted in number of MP per kilo salt (MP/kg) at left and concentrations per kilo salt ( $\mu\text{g}/\text{kg}$ ) at right. Grey dots are single measurements. The y-axes are logarithmic.

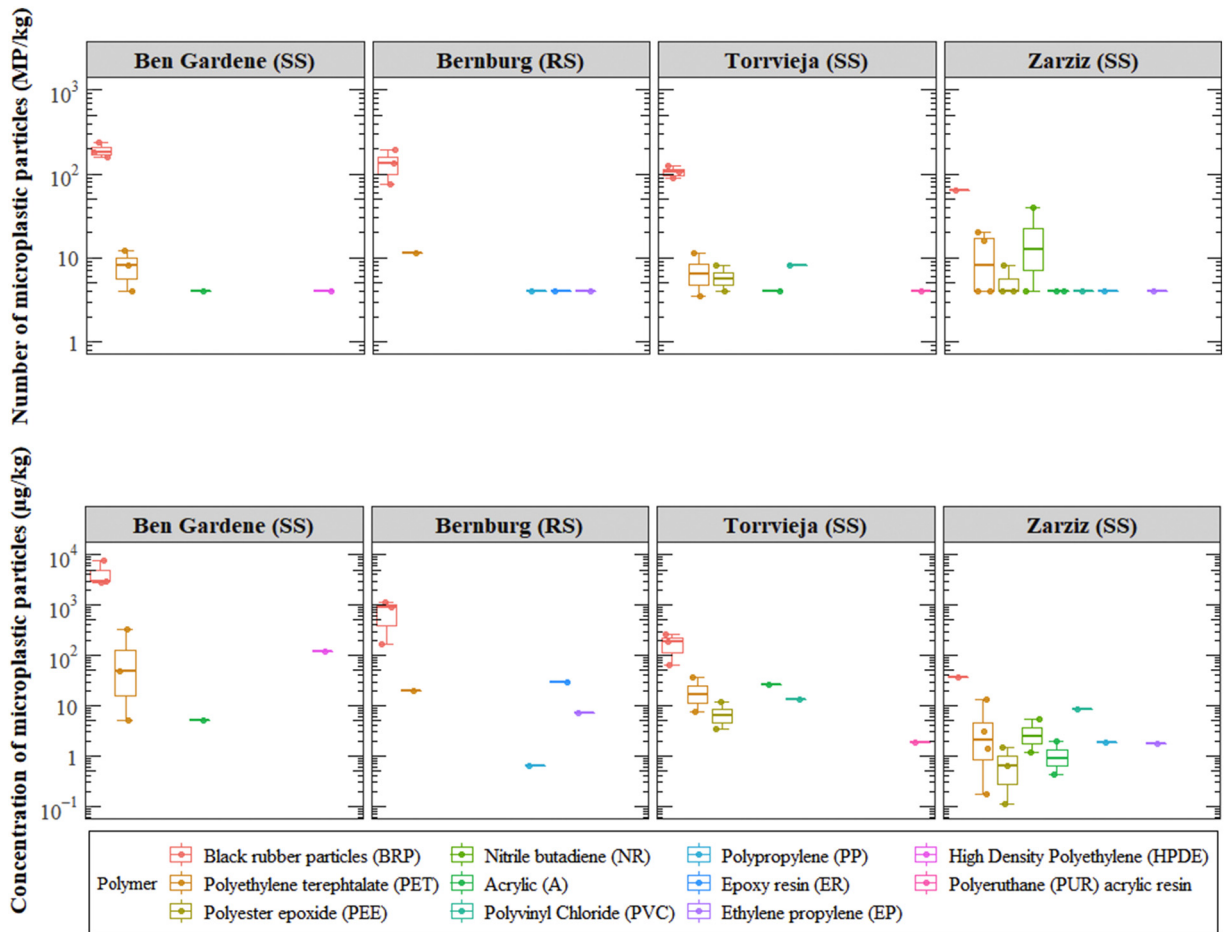


**Fig. 6.** Box-plot showing the distribution of microplastic fibres and fragments per kilo salt found at each site, by polymer type (above) and the mean concentration of microplastic fibres and fragments found at each site, by polymer type (below). Polymer types: Black rubbery particles, polyethylene terephthalate (PET), acryl (A), epoxy resin (ER), ethylene propylene (EP), polyester epoxide (PEE), polyvinyl chloride (PVC, non-black particles), high-density polyethylene (HDPE), nitrile butadiene (NR), polyurethane (PUR) acrylic resin, polypropylene (PP).

the statistical analysis using multivariate tools showed no significant difference between the rock salt and sea salt in this study with regards to microplastic particles, the salt types for this calculation are taken into consideration. From this analysis we estimate that road salt used on state and county roads contributes to a total of 0.15 t of MPs per year (tonnes/year) in Norway, which is 0.23 grams per kilometre road

(g/km). This is equivalent to 0.003% of the total release of RAMP. In Sweden and Denmark, the release of MPs from road salt is 0.07 t/year (0.07 g/km) and 0.03 t/year (0.04 g/km), respectively. This is equivalent to 0.008% of RAMP in Sweden and 0.0004–0.0008% of RAMP in Denmark. Summary of the calculations are presented in the supporting information (Table S4).

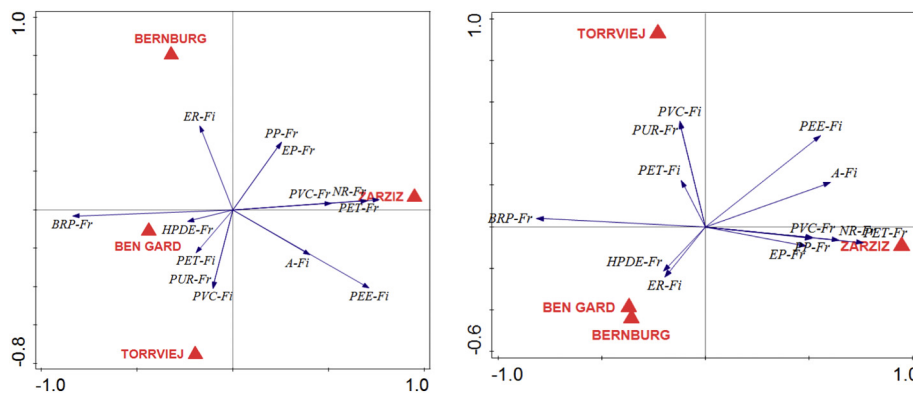


**Fig. 7.** The figure shows the constrained RDA plot of the variation of polymer types (arrows; Black rubber particles (BRP), Polyethylene terephthalate (PET), Polyester epoxide (PEE), Nitrile butadiene (NR), Acrylic (A), Polyvinyl chloride (PVC), Polypropylene (PP), Epoxy resin (ER), Ethylene propylene (EP). Fi = fibres and Fr = fragments) when using “sample sites” as the explanatory variable (triangular shapes; Torrvieja, Zorziz, Ben Gardene and Bernburg). In the left plot, the number of particles per polymers is used and in right plot, the concentration of polymers (% of total) is used. The arrow points in the direction of steepest increase of the polymer type. A sharp angle between the arrows indicate positive correlation, while arrows going in opposite direction indicate negative correlation. Angle close to 90 degrees indicate no correlation.

## 4. Discussion

### 4.1. Road de-icing salt compared to RAMP

Based on the results in the present study, road salt seems to be a negligible source of road-related microplastic pollution compared to other main sources, and especially compared to the contribution from car tires. It is, however, important to underline that the estimation of total RAMP emissions in Norway (Sundt et al., 2014; Sundt et al., 2016; Vogelsang et al., 2018) is based on the total annual distance travelled for different vehicle types, and does not distinguish between state, county, municipal or other roads (Vogelsang et al., 2018). In Sweden, the RAMP emissions are for roads open to the public only (Magnusson et al., 2017), meaning that they are excluding all private roads from their calculations. For Denmark there is no information on what types of roads they have included in the emission calculations (Lassen et al., 2015). This study, on the other hand, has calculated the emission of MPs from road salt emitted from state and county roads only. Although a large proportion of the road network that uses road salt will be either state or county roads, there are also municipal roads, especially in larger cities like Oslo and Stockholm, where road salt is widely used. There might also be other roads where winter and road conditions require that road salt is used to ensure traffic safety. Additionally, road salt (e.g.  $\text{CaCl}_2$  or  $\text{MgCl}_2$ ) is also applied on gravel roads in summer to prevent air dust during dry weather conditions. However, these numbers are difficult to obtain, as there are different road owners and no common reporting platform for road salt use. In Norway, state and county roads combined have a total length of 62,923 km, municipal roads of 44,048 km and private roads 100,384 km (Statens vegvesen, 2019b). Many smaller roads, both county and municipal, are not salted during winter as other winter maintenance measures are preferred (e.g. the roads are just ploughed and sanded). It should be clearly stated that the emission calculation is associated with relatively large uncertainties. These arise because it is based on calculated concentrations, a small sample size compared to the total salt emission, as well as a varying salt consumption per year. In addition, the salt used in this study comes from only one salt importer. Even though they are one of the major importers of salt to all three countries, there may also be other salt importers using other salt production sites. Future studies should aim to investigate road salt from other sources and calculate the emission of microplastic particles from road salt in other countries, especially countries with high road salt emissions such as USA, Canada and China.

### 4.2. Black rubbery particles

In the present work, we suggest that the sources of BRPs are conveyor belts, which are used at all salt production sites included in this study (Rieber, 2019). The belts are in general made of thermoplastic materials with carbon black added for durability. There are probably several different thermoplastics used in conveyor belts, determined by the different applications of the conveyor belt and the manufacturers. However, according to a U.S. patent (Van and Ter, 1990) from 1990, conveyor belts used within mining industries use PVC. No specific information on the types of conveyor belts used at the salt production sites could be obtained. However, since rock salt originates from salt mines it is likely that the conveyor belts used in salt production is of similar type to those used for other mining activities. Upon visual examination using microscope and forceps, the BRPs identified in rock salt did not differ from the ones found in sea salt (Fig. 3), which supports the assumption that they originate from the same material. Since we also found a presence of SBR in the Ben Gardene sample, it is a possibility that some of the BRP could come from tire wear, as well as both trucks, lorries, tractors and other vehicles may be used at production sites of both sea salt and rock salt. Even though they did not display similar characteristic shape as tire particles in other studies (Kreider et al., 2010), they might also be made of different types of tires and not

subjected to the harsh road climate in which other tire particles are assumed to be infused with road wear particles.

### 4.3. Comparison with other studies

In total, the number of particles found for both sea salt and rock salt were comparable to some studies on food-grade salt, although a large variation in number of MPs is reported in the different studies (Table S5). In this study, sea salt was found to have  $35 \pm 60$  MP/kg, ranging from 32 to 252 MP/kg. In the food-grade salt studies, the number of MPs found differ between n.d. MP/kg and 16,329 MP/kg. One of the food-grade salt studies also included Spanish sea salts from the Mediterranean (Iniguez et al., 2017). In this study, the number of MPs from the Mediterranean samples ranged from 60 to 280 MP/kg. Two brands of sea salt were collected from Murcia, which is close to Torrevieja. The mean number of MPs from Murcia was  $280 \pm 3$  MP/kg and  $105 \pm 7$  MP/kg. In comparison, the mean number of MPs found for the Torrevieja site in our study was  $36 \pm 49$  MP/kg. The mean number of MPs in rock salt in the present study was  $61 \pm 76$  MP/kg. Our result corresponds well to the results found for food-grade rock salt, which was  $38 \pm 55$  MP/kg (Kim et al., 2018) and  $12 \pm 1$  MP/kg (Gündoğdu, 2018). Only two other studies reported concentrations of microplastic particles in sea salt. However, they represent sea salt from different oceans. The concentrations varied between n.d. and 46.5 mg/kg salt (Kim et al., 2018; Seth and Shrivastav, 2018). The Mediterranean Sea salts ranged from 0.5–2.4 mg/kg, which corresponds well to the findings of this study ( $442 \pm 1466$  µg/kg). Although the results of the present study are comparable to previous salt studies, the fact that different methods have been used, both in preparation and analysis, needs to be addressed. As for a large proportion of microplastic studies, the lack of consistency in methodologies or standardisation is an obvious issue of concern. In the food-grade salt studies, the pore size used to retain the MPs after dissolving the salts differed between 0.2 and 5 µm for all studies except one where they used the pore size 149 µm (Karami et al., 2017), thus excluding all particles <149 µm from their samples. The reason for this is not sufficiently explained and as this study also reported a very low range of MPs (n.d.–10 MP/kg), the pore size used is an obvious issue when comparing studies. For the other studies where pore sizes of 0.2–5 µm were applied, a consistent use of the same pore size would be beneficial when comparing results. However, they have all used pore sizes that will retain particles that are at least 5 µm in size, and using visual techniques such as microscopes, FT-IR (Iniguez et al., 2017; Kim et al., 2018; Lee et al., 2019; Seth and Shrivastav, 2018; Yang et al., 2015) or Raman spectroscopy (Gündoğdu, 2018; Karami et al., 2017), the lower limit of detection depends on the lower limit of the analysis. One of the food-grade salt studies (Renzi and Blašković, 2018) was excluded from comparison with our results because they did not apply chemical analysis of the polymer content to confirm the presence of MPs, and they reported the largest variation in the salt studies (20–19,820 MP/kg).

The main difference between production of food grade salt and road salt, is that the food grade salt goes through a double washing process at the production site whereas the road salt is only subjected to a single washing process (Rieber, 2019). None of the other salt studies have reported the presence of “black rubbery particles”, large concentrations of PVC or tire particles/SBR. As our study shows such a high abundance, we can only hypothesize why it was not identified in other studies. One reason might be the extra washing step that is used for food grade salts. There might also be other refining steps when processing salt for the food market, compared to salt used for industrial purpose.

Considering all MPs except the BRPs, road salt is considerably less contaminated compared to both sea salts and rock salts used for food. A suggested reason for this finding might be that the road salt used for this study has never been packaged and came directly from bulk samples at the importer's storage site. The Torrevieja-sample had also been transported in bulk like the other salts in the study, but we

received it in a plastic bag-package meant for commercial sale, packed in Norway. This bag was made of PE (see Figs. S1–S3), and no PE was found in the salts from Torreveija. We can therefore disregard that the microplastics in the Torreveija-samples came directly from the packaging. In comparison to our samples, most food grade salts are packed in bulk bags for shipment and then repacked in smaller packages for different salt brands (Rieber, 2019). Such bulk bags (for example “Flexible intermediate bulk container, FIBC”) are commonly made from woven polyethylene PE or PP (Diffpack, 2020), which might explain why both PE and PP fibres are found in high numbers in the salt used for food (Gündoğdu, 2018; Iniguez et al., 2017; Karami et al., 2017; Kim et al., 2018; Lee et al., 2019; Seth and Shrivastav, 2018; Yang et al., 2015), and less in the road salt. PET is commonly used in packaging, as well as one of the most used synthetic fibres in the textile industry, thus it is not surprising that PET was the second most abundant polymer found in the road salt samples, after BRP. PET is also found in high abundance in the studies of food-grade salt (Gündoğdu, 2018; Iniguez et al., 2017; Karami et al., 2017; Kim et al., 2018; Seth and Shrivastav, 2018; Yang et al., 2015).

It has been suggested that PET is more abundant than other polymer-types in food-grade salt due to its higher density (1.34–1.39 g/cm<sup>3</sup>) (Bråte et al., 2017) compared to PE (Low density PE: 0.92 g/cm<sup>3</sup>, High density PE: 0.95 g/cm<sup>3</sup>) (Polymer Science, 2020) and PP (Bråte et al., 2017) (0.90–0.92 g/cm<sup>3</sup>), causing PET to more easily follow the salt during the production process (Iniguez et al., 2017; Yang et al., 2015). In the present study, BRP were the most abundant particle. Using the results from the Pyrolysis GC–MS, we can assume that most of the BRPs are made of PVC, as PVC was found to be the polymer with the largest mass in the Ben Gardene sample. As we stated in this study, most BRPs are of PVC, they would have a density of 1.160–1.3 g/cm<sup>3</sup> (Bråte et al., 2017), with a high carbon black content (1.8–2.1 g/cm<sup>3</sup>) (INCHEM, 2017). It is likely that these particles will have a higher density than the other polymers found, and therefore be accumulated with the salt. Each brand of salt might also have different purification processes for their salt before it is packaged and released to the food market. The road salt is commonly transported in bulk containers, using conveyer belts up until the very last step of the transportation. This might explain why we find so much of these black rubber particles in this study compared to none being detected in the previous salt studies.

#### 4.4. Limitations of the methodology

In the present study the lowest limit of detection is related to the lowest sizes of particles that could be handled with forceps and transferred to either ATR-FTIR or  $\mu$ FTIR windows. Using the longest axis of the particles as the length, the smallest detected particle that was possible to transfer to the FT-IR compression cell and get a match score (>0.6) from was 59  $\mu$ m long (and 37  $\mu$ m wide). However, particles as small as 21  $\mu$ m (longest axis) were detected on filters and included in this dataset, as it had matching morphology to BRP. So, for this study and the methods used, it was not possible to detect particles below 21  $\mu$ m, although there might be particles <21  $\mu$ m present. In this study, GF-filters with pore size 1.6  $\mu$ m was used. However, for the analysis using visual methods, the pore size used has less of an impact as long as it is lower than the smallest particle size possible to detect on the filter papers and measure using the FTIR. For the Pyrolysis GC–MS on the other hand, the pore size used can have a larger impact on the results. Using Pyrolysis GC–MS makes it possible to detect even small amounts of polymers if the mass of these particles in total is above the LOQ for the Pyrolysis GC–MS method. This is demonstrated in our sample from Ben Gardene where we found low concentrations of PS and PP in the sample via GC–MS but did not detect particles via the visual analysis. We were also able to detect and measure the concentration of SBR in the sample, which corresponds to some of the BRP being tire

particles. On the other side, if we do have a number of very small particles of a specified polymer in the sample and a few quite large particles (<5 mm) of the same polymer, the presence of the small particles will be masked in the total amount of polymers and likely not contribute that much to the total mass. This also means that the information on sizes will be lost. This can be adjusted using filters with different pore sizes as well as sieves to separate the sample in size fractions. This will contribute to more data on the mass of polymers related to size fractions, which may be of value, and should be considered in future studies. The use of Pyrolysis GC–MS also allows for the detection of nanoplastics if the filters with appropriate pore sizes to retain particles in the nanoscale are used and if the measurements are above the LOQ.

As shown in this study, the mass of polymers found using visual techniques and concentration calculation corresponded well to the mass found using Pyrolysis GC–MS. In the visual analysis, three groups of polymers were detected; BRP (suspected PVC), PET and PE. This complies with results from the Pyrolysis GC–MS where PVC, PET and PE had the highest, second highest and third highest concentration in the sample, respectively. This validates that visual analysis together with FT-IR can be used to calculate concentrations of different polymers from a sample, not just the number of particles. However, this is of course limited to what the FT-IR can analyse, and as shown in this study, particles with a high carbon black content can prove difficult to analyse via FTIR.

## 5. Conclusions

The concentration of MP in rock salt and sea salt used for de-icing of winter roads was low. The estimated annual release of MPs from road de-icing salt is considerably lower than the estimated release coming from other known MP sources in Norway. Based on the current study, the application of road salt for de-icing of winter roads is a negligible source of microplastic to the environment. It is likely that the MPs found in sea salt are due to both contaminated sea water and contamination through processing. This needs to be further investigated in order to reduce the contamination of salts used for road purposes. As only one rock salt site was included in this study, we propose that future studies on road salt should include different rock salt sites for comparison with the sea salt, as well as include data for municipal roads in new estimates. We also suggest that future studies should include more detailed analysis of the “black rubbery particles”, for example by employing Pyrolysis GC–MS, as well as employing Pyrolysis GC–MS in a wider scale to investigate the presence of small microplastics and nanoplastics in the salt samples.

## Declaration of competing interest

The authors declare that they have no known competing financial interests or personal relationships that could have appeared to influence the work reported in this paper.

## Acknowledgements

We would like to thank Rachel Hurley and Nina Buenaventura (NIVA) for guidance on visual analysis and FTIR. We would also like to thank Amy Lusher and Emelie Skogsberg (NIVA) for valuable comments to the manuscript.

## Funding sources

This work was funded in collaboration between the Norwegian Institute for Water Research (NIVA) and the NordFoU-project REHIRUP, consisting of the Norwegian Public Roads Administration, the Swedish Transport Administration and the Danish Road Directorate. Part of the



work is also supported by the Research Council of Norway through its Centres of Excellence funding scheme, project number 223268/F50.

## Author contributions

The manuscript was written through contributions of all authors. All authors have given approval to the final version of the manuscript.

## Appendix A. Supplementary data

Supplementary data to this article can be found online at <https://doi.org/10.1016/j.scitotenv.2020.139352>.

## References

- Andrady, A.L., 2011. Microplastics in the marine environment. *Mar. Pollut. Bull.* 62, 1596–1605.
- Braak, C.J.Ft, Šmilauer, P., 2018. *Canoco Reference Manual and User's Guide: Software for Ordination (Version 5.10)*. Biometris, Wageningen University & Research, Wageningen.
- Bråte, I.L.N., Huwer, B., Thomas, K.V., Eidsvoll, D.P., Halsband, C., Almroth, B.C., et al., 2017. *Micro- and Macro-plastics in Marine Species From Nordic Waters*. Nordic council of Ministry Report.
- CIA, 2017. *Statistics of road network*. <https://www.cia.gov/library/publications/the-world-factbook/fields/385.html>.
- Demers, C.L., 1992. Effects of road deicing salt on aquatic invertebrates in four Adirondack streams. *Chemical Deicers and the Environment*. Lewis Publishers, Boca Raton, Florida, USA, pp. 245–251.
- Diffpack, 2020. FIBC.
- Eisenbraun, P., Dümichen, E., Ruhl, A.S., Jekel, M., Albrecht, M., Gehde, M., et al., 2018. Two birds with one stone—fast and simultaneous analysis of microplastics: microparticles derived from thermoplastics and tire wear. *Environ. Sci. Technol. Lett.* 5, 608–613.
- Environment Canada, 2012. *Five-year Review of Progress: Code of Practice for the Environmental Management of Road Salts (Report published March 31, 2012)*.
- Fay, L., Shi, X., 2012. Environmental impacts of chemicals for snow and ice control: state of the knowledge. *Water Air Soil Pollut.* 223, 2751–2770.
- Findlay, S.E.G., Kelly, V.R., 2011. Emerging indirect and long-term road salt effects on ecosystems. *Ann. N. Y. Acad. Sci.* 58–68.
- Frias, J.P.G.L., Gago, J., Otero, V., Sobral, P., 2016. Microplastics in coastal sediments from southern Portuguese shelf waters. *Mar. Environ. Res.* 114, 24–30.
- GESAMP, 2016. *Sources, fate and effects of microplastics in the marine environment: part two of a global assessment*. Joint Group of Experts on the Scientific Aspects of Marine Environmental Protection, p. 220.
- Government of Canada, 2018. *Statistics of road network*. <https://www.tc.gc.ca/eng/policy/transportation-canada-2018.html#item-10>.
- Grigoratos, T., Martini, G., 2014. Non-exhaust traffic related emissions. Brake and tyre wear PM. *JRC Science and Policy Reports*, p. 53.
- Gündoğdu, S., 2018. Contamination of table salts from Turkey with microplastics. *Food Addit. Contam. Part A* 35, 1006–1014.
- Hann, S., Sherrington, C., Jamieson, O., Hickman, M., Bapasola, A., 2018. In: Sherrington, C. (Ed.), *Investigating Options for Reducing Releases in the Aquatic Environment of Microplastics Emitted by Products*. Eunomia.
- Hermabessiere, L., Himber, C., Boricaud, B., Kazour, M., Amara, R., Cassone, A.-L., et al., 2018. Optimization, performance, and application of a pyrolysis-GC/MS method for the identification of microplastics. *Anal. Bioanal. Chem.* 410, 6663–6676.
- INCHEM, 2017. *Carbon Black*. 2020. European Commission.
- Iniguez, M.E., Conesa, J.A., Fullana, A., 2017. Microplastics in Spanish table salt. *Sci. Rep.* 7, 121396:2017, 2017. Rubber – Determination of Mass Concentration of Tire and Road Wear Particles (TRWP) in Soil and Sediments – Pyrolysis-GC/MS Method. International Organization for Standardization, Genève, Switzerland.
- Karami, A., Golieskardi, A., Choo, C.K., Larat, V., Galloway, T.S., Salamatinia, B., 2017. The presence of microplastics in commercial salts from different countries. *Sci. Rep.* 7, 121396:2017, 2017. Rubber – Determination of Mass Concentration of Tire and Road Wear Particles (TRWP) in Soil and Sediments – Pyrolysis-GC/MS Method. International Organization for Standardization, Genève, Switzerland.
- Karraker, N.E., Gibbs, J.P., Vonesh, J.R., 2008. Impacts of road deicing salt on the demography of vernal pool-breeding amphibians. *Ecol. Appl.* 18, 724–734.
- Ke, C., Li, Z., Liang, Y., Tao, W., Du, M., 2013. Impacts of chloride de-icing salt on bulk soils, fungi, and bacterial populations surrounding the plant rhizosphere. *Appl. Soil Ecol.* 72, 69–78.
- Kelly, V.R., Findlay, S.E.G., Weathers, K.C., 2019. *Road Salt: The Problem, the Solution, and How to Get There*. Cary Institute of Ecosystem Studies (Report, 16 pages).
- Kim, J.-S., Lee, H.-J., Kim, S.-K., Kim, H.-J., 2018. Global pattern of microplastics (MPs) in commercial food-grade salts: sea salt as an indicator of seawater MP pollution. *Environ. Sci. Technol.* 52, 12819–12828.
- Kreider, M.L., Panko, J.M., McAtee, B.L., Sweet, L.L., Finley, B.L., 2010. Physical and chemical characterization of tire-related particles: comparison of particles generated using different methodologies. *Sci. Total Environ.* 408, 652–659.
- Lassen, C., Hansen, S.F., Magnusson, K., Hartmann, N.B., Rehne Jensen, P., Nielsen, T.G., et al., 2015. *Microplastics: Occurrence, Effects and Sources of Releases to the Environment in Denmark*. Danish Environmental Protection Agency.
- Lee, H., Kunz, A., Shim, W.J., Walther, B.A., 2019. Microplastic contamination of table salts from Taiwan, including a global review. *Sci. Rep.* 9, 10145.
- Lusher, A.L., McHugh, M., Thompson, R.C., 2013. Occurrence of microplastics in the gastrointestinal tract of pelagic and demersal fish from the English Channel. *Mar. Pollut. Bull.* 67, 94–99.
- Lusher, A.L., Welden, N.A., Sobral, P., Cole, M., 2017. Sampling, isolating and identifying microplastics ingested by fish and invertebrates. *Anal. Methods* 9, 1346–1360.
- Magnusson, K., Eliasson, K., Fråne, A., Haikonen, K., Hultén, J., Olshammar, M., et al., 2017. *Swedish Sources and Pathways for Microplastics to the Marine Environment: A Review of Existing Data*. IVL Swedish Environmental Research Institute.
- Marsalek, J., 2003. Road salts in urban stormwater: an emerging issue in stormwater management in cold climates. *Water Sci. Technol.* 48, 61–70.
- MSFD Technical Subgroup on Marine Litter, 2013. *Guidance on Monitoring of Marine Litter in European Seas*. European Commission, Joint Research Centre, Institute for Environment and Sustainability.
- Okoffo, E.D., Ribeiro, F., O'Brien, J.W., O'Brien, S., Tschärke, B.J., Gallen, M., et al., 2020. Identification and quantification of selected plastics in biosolids by pressurized liquid extraction combined with double-shot pyrolysis gas chromatography–mass spectrometry. *Sci. Total Environ.* 715, 136924.
- Polymer Science, 2020. *Polymer properties database*. URL: <http://www.polymerdatabase.com>.
- Primpke, S., Wirth, M., Lorenz, C., Gerdt, G., 2018. Reference database design for the automated analysis of microplastic samples based on Fourier transform infrared (FTIR) spectroscopy. *Anal. Bioanal. Chem.* 410, 5131–5141. <https://doi.org/10.1007/s00216-018-1156-x>.
- Renzi, M., Blašković, A., 2018. Litter & microplastics features in table salts from marine origin: Italian versus Croatian brands. *Mar. Pollut. Bull.* 135, 62–68.
- Rieber, G., 2019. *Personal Communication on the Different Salt Production Sites and Practices Used for Road Salt*.
- Rochman, C.M., 2018. Microplastics research—from sink to source. *Science* 360, 28–29.
- Rochman, C.M., Brookson, C., Bikker, J., Djuric, N., Earn, A., Bucci, K., et al., 2019. Rethinking microplastics as a diverse contaminant suite. *Environ. Toxicol. Chem.* 38, 703–711.
- RStudio, 2019. *RStudio: Integrated Development for R*. RStudio, Inc, Boston, MA.
- Schuler, M.S., Relyea, R.A., May 2018. A review of the combined threats of road salts and heavy metals to freshwater systems. *BioScience* 68 (5), 327–335. <https://doi.org/10.1093/biosci/biy018>.
- Seth, C.K., Shrivastava, A., 2018. Contamination of Indian sea salts with microplastics and a potential prevention strategy. *Environ. Sci. Pollut. Res.* 25, 30122–30131.
- Simon, M., van Alst, N., Vollertsen, J., 2018. Quantification of microplastic mass and removal rates at wastewater treatment plants applying focal plane Array (FPA)-based Fourier transform infrared (FT-IR) imaging. *Water Res.* 142, 1–9.
- Statens vegvesen, 2019a. *Hvor mye salt brukes i Norge?* Updated January 2019. <https://www.vegvesen.no/fag/veg+og+gate/drift+og+vedlikehold/Vinterdrift/salting/sporsmal-og-svar/hvor-mye-salt>.
- Statens vegvesen, 2019b. *Road statistics from the road map applications Vegkart*. <https://vegkart.atlas.vegvesen.no/>, Accessed date: 8 May 2020.
- Sundt, P., Schulze, P.-E., Syversen, F., 2014. Sources of Microplastic-pollution to the Marine Environment. p. 86.
- Sundt, P., Syversen, F., Skogedal, O., Schulze, P.-E., 2016. Primary Microplastic-pollution: Measures and Reduction Potentials in Norway. p. 117.
- Tiwari, A., Rachlin, J.W., 2018. A review of road salt ecological impacts. *Northeast. Nat.* 25, 123–142, 20.
- Trafikverket, 2017. *Statistics over Swedish road network*. <https://www.trafikverket.se/resa-och-trafik/vag/Sveriges-vagnat/>.
- Trafikverket, 2019. *Vägverkets saltförbrukning säsongerna 1976/77–2017/18*.
- US Department of Transportation, 2017. *Statistics of road network*. <https://www.fhwa.dot.gov/policyinformation/statistics/2016/hm12.cfm>.
- Van, C., Ter, B., 1990. *Conveyor Belt of PVC Provided with a Compound Layer of Reinforcing Material and a Process of Weaving Said Reinforcing Layer*, United States.
- Vejdirektoratet, 2019a. *Saltforbrug og antal udkald på statvejnettet*. p. 2019.
- Vejdirektoratet, 2019b. *Statistics over Danish road network*. <https://www.dst.dk/da/Statistik/emner/geografi-miljoe-og-energi/infrastruktur/vejnet>.
- Vogelsang, C., Lusher, A.L., Dadkhah, M.E., Sundvor, I., Umar, M., Ranneklev, S.B., et al., 2018. Microplastics in Road Dust – Characteristics, Pathways and Measures.
- Wagner, S., Huffer, T., Klockner, P., Wehrhahn, M., Hofmann, T., Reemtsma, T., 2018. Tire wear particles in the aquatic environment – a review on generation, analysis, occurrence, fate and effects. *Water Res.* 139, 83–100.
- Wickham, H., 2009. *ggplot2: Elegant Graphics for Data Analysis*. Springer, New York.
- Wik, A., Dave, G., 2009. Occurrence and effects of tire wear particles in the environment – a critical review and an initial risk assessment. *Environ. Pollut.* 157, 1–11.
- Yang, D.Q., Shi, H.H., Li, L., Li, J.N., Jabeen, K., Kollandhasamy, P., 2015. Microplastic pollution in table salts from China. *Environ. Sci. Technol.* 49, 13622–13627.